metals

MDPI

Article

Effect of V_2O_5 on Consolidation, Reduction, and Softening-Melting Behavior of High-Cr Vanadium Titanomagnetite

Jianxing Liu [1,2], Zhenxing Xing [1,2,*], Xuyang Wang [1], Gongjin Cheng [1,2] and Xiangxin Xue [1,2]

[1] School of Metallurgy, Northeastern University, Shenyang 110819, China
[2] Liaoning Key Laboratory of Recycling Science for Metallurgical Resources, Shenyang 110819, China
* Correspondence: zhxing_x@163.com

Abstract: Vanadium titanomagnetite is an important mineral resource. It is a raw material for iron-making, vanadium extraction, strategic metal titanium production, and titanium dioxide production. In this study, high chromium vanadium titanomagnetite (High-Cr VTM) and ordinary iron ore were used as raw materials for pelletizing. The effect of V_2O_5 on the preparation and properties of High-Cr VTM pellets was studied. The influence of V_2O_5 on the properties of the green pellets, the compressive strength of oxidized pellets, the reduction swelling index and reduction degree, softening-melting behavior, and the migration law of Fe, Ti, and Cr in the reduction process were studied by X-ray diffraction (XRD) and scanning electron microscopy (SEM). The results show that with the increase in V_2O_5 content, the properties of the green pellets basically showed a trend of first decreasing and then increasing but all met the basic requirements of pelletizing. When the added amount of V_2O_5 in the pellet was 6%, the compressive strength of the oxidized pellet was the lowest at only 2565 N/pellet but it still met the quality requirements for pellets in blast furnace production. As the dosage of V_2O_5 increased, the reduction swelling index and reduction degree of the pellets showed a trend of first increasing and then decreasing. The addition of V_2O_5 can increase the softening initial temperature, softening final temperature, melting start temperature, and dripping temperature of the High-Cr VTM pellets, narrowing the softening interval, and expanding the melting dripping interval. The experimental results provided a data reference for revealing the influence of V_2O_5 on High-Cr VTM pellets during the blast furnace smelting process.

Keywords: high-Cr VTM; V_2O_5; pellet; reduction; softening-melting

Citation: Liu, J.; Xing, Z.; Wang, X.; Cheng, G.; Xue, X. Effect of V_2O_5 on Consolidation, Reduction, and Softening-Melting Behavior of High-Cr Vanadium Titanomagnetite. *Metals* **2023**, *13*, 1171. https://doi.org/10.3390/met13071171

Academic Editor: Mark E. Schlesinger

Received: 22 May 2023
Revised: 19 June 2023
Accepted: 20 June 2023
Published: 23 June 2023

1. Introduction

Vanadium has excellent physical and chemical properties and is known as the vitamin of metals. In steel smelting, vanadium can refine the structure and grains of steel, increase the grain-coarsening temperature, and increase the strength, toughness, and wear resistance of steel [1–4]. With the development of science and technology, the demand for new materials is also increasing day by day. The application of vanadium in non-steel fields is becoming increasingly widespread, covering various fields such as aerospace, chemistry, batteries, pigments, glass, optics, medicine, etc. [5,6].

China is rich in vanadium titanomagnetite (VTM) resources, with proven reserves of more than 38 billion tons, ranking fourth in the world [7,8]. Panzhihua in the Sichuan Province, Chengde in Hebei Province, and Chaoyang in Liaoning Province are the main distribution areas of vanadium titanomagnetite resources in China [9,10]. Among them, the vanadium titanomagnetite deposits in the Panxi area are large in scale and relatively concentrated in distribution, with potential iron ore reserves of nearly 11.77 billion tons, including 13.386 million tons of vanadium (V_2O_5), accounting for 58% of the national vanadium reserves; titanium (TiO_2) is 35.526 million tons, accounting for 90.54% of the national titanium reserves [11,12].

Tang et al. [13,14] found that the compressive strength of finished pellets decreased with the increase in the content of High-Cr VTM but the reduction in the swelling performance of pellets could be improved. Zhang et al. [15,16] studied the soft-melt dripping performance of the High-Cr VTM sinter under different basicity. The results indicated that increasing the basicity of the sinter could significantly improve the smelting efficiency of blast furnaces. Cheng et al. [17–19] studied the influence of valuable components on the compressive strength, the reduction swelling index, and soft-melt dropping performance of High-Cr VTM pellets by adding CaO, Cr_2O_3, and TiO_2 to the High-Cr VTM pellets. The results indicated that CaO had a significant impact on the compressive strength of pellets. As the mass fraction of Cr_2O_3 increased, the softening temperature of the pellets showed an upward trend. With the increase in TiO_2 content, the compressive strength of the pellets was significantly improved, and the difficulty of soft-melt dripping also increased.

High-Cr VTM is a vanadium titanomagnetite with special complexity in raw materials, composition, distribution, and grade [20–24]; therefore, it is more difficult to smelt than ordinary iron ore, so it has not been effectively developed and utilized. In order to realize the comprehensive utilization of High-Cr VTM, it is necessary to study the influence of vanadium, titanium, and chromium on the smelting of High-Cr VTM [25–27]. Therefore, in this study, the effects of V_2O_5 dosage on the drop strength, compressive strength, reduction swelling index, reduction degree, and softening-melting behavior of pellets were studied. On this basis, the influence of V_2O_5 dosage on the phase composition and microstructure of oxidized and reduced pellets was discussed.

2. Experimental Methods

2.1. Raw Materials

The raw materials used in this experiment include High-Cr VTM, ordinary iron ore, and V_2O_5 (AR, Sinopharm Group, China). The chemical composition of High-Cr VTM and ordinary iron ore is shown in Table 1. The experiment used bentonite as the binder, and its chemical composition is shown in Table 2.

Table 1. Chemical composition of the experimental raw materials (mass/%).

Compositions	TFe	FeO	V_2O_5	TiO_2	Cr_2O_3	CaO	SiO_2	MgO	Al_2O_3	S
High-Cr VTM	55.44	27.27	0.35	10.88	0.53	0.62	2.60	2.60	2.28	0.37
Ordinary iron ore	67.22	25.99	/	/	/	0.14	5.63	0.26	0.23	0.06

Table 2. Chemical compositions of bentonite (mass/%).

Compositions	SiO_2	Al_2O_3	MgO	CaO	Na_2O	K_2O	LOI
Content	67.45	14.47	4.61	2.47	1.68	1.19	8.13

2.2. Experimental Methods

A mixture of 40% high-chromium vanadium titanium magnetite and 60% common iron ore was mixed with 0%, 3%, 6%, and 9% mass fraction of V_2O_5 and 1% mass fraction of bentonite as a binder, with 7% water added to the mixture. The mixture was made into 10–14 mm green pellets by disc granulator, and the performance was tested and analyzed. The green pellets were dried in an oven and oxidized in a muffle furnace. The dried green pellets were first placed in a muffle furnace at a constant temperature of 900 °C for 20 min, then the preheated pellets were removed and placed in a muffle furnace at 1300 °C for oxidation and roasting for 20 min. The compressive strength of the oxidized pellets was tested by a digital display automatic pellet pressure tester.

Eighteen oxidized pellets with a particle size of about 12 mm and regular volume without cracks were selected as the samples of this experiment. After the oxidized pellets were heated to 900 °C in an inert atmosphere, the reducing atmosphere was adjusted to 10.5 L/min N_2 and 4.5 L/min CO. After 60 min of reduction, the pellets were cooled to ambient temperature in an inert atmosphere. Formula (1) was used to calculate the reduction swelling index, expressed as the percentage of volume:

$$RSI = \frac{V_t - V_0}{V_0} \times 100\% \quad (1)$$

where V_0 is the average volume of the sample before reduction (mm^3); V_t is the average volume of the sample after reduction (mm^3); RSI is the reduction swelling index (%).

Then, 500 g of oxidized pellets were selected as the sample for the reduction experiment. After the oxidized pellets were heated to 900 °C under an inert atmosphere, the reducing atmosphere was adjusted to 10.5 L/min N_2 and 4.5 L/min CO. After 180 min of reduction, the pellets were cooled to ambient temperature under an inert atmosphere. Formula (2) was used to calculate the reduction degree index (RI) of pellets after reduction for 180 min.

$$f = \left[\frac{0.111W_1}{0.430W_2} + \frac{m_1 - m_2}{m_1 \times 0.430W_2} \times 100\right] \times 100\% \quad (2)$$

where m_1 is the mass of the sample before reduction (g); m_2 is the mass of the sample after 180 min reduction (g); W_1 is the content of FeO in the sample before the test (mass%); W_2 is the total iron content of the sample before the test (mass%); and f is the reduction index (%).

Figure 1 shows the equipment diagram of the softening-melting process. The equipment is composed of a heating furnace, automatic control system, and data recording system. The particle size of coke and oxidized pellets was required to be 10~12.5 mm. In order to simulate the BF melting conditions, it was necessary to first lay coke particles with a thickness of 30 mm at the bottom of the graphite crucible, with a mass of about 74 g. After being flattened, 500 g of oxidized pellets were placed into the crucible and then laid with coke with a thickness of 15 mm at the top of the sample, with a mass of about 38 g. The graphite crucible with the pressure rod was placed smoothly into the reduction tube and the thermocouple was connected. Then, the external pressure made the displacement sensor drop and pressed on the pressure rod smoothly. During the experiment, the pressure was adjusted according to the load setting of the descending process of the charge. The lower part of the reduction tube should be well sealed during operation to ensure the accuracy of differential pressure measurement during the experiment. The temperature regime and atmosphere changes in the experiment are shown in Figure 2. In this experiment, the initial softening temperature (T_4) and the final softening temperature (T_{40}) are the corresponding temperatures when the shrinkage rate of the charge reached 4% and 40%, respectively, and the softening interval was the difference between T_{40} and T_4. Melting start temperature (T_S) refers to the temperature when the pressure difference of the charge begins to shake up in the process of reducing the melting drop, T_D was the drop temperature, and the drop interval (T_D-T_S) was the difference between the drop temperature and the melting start temperature.

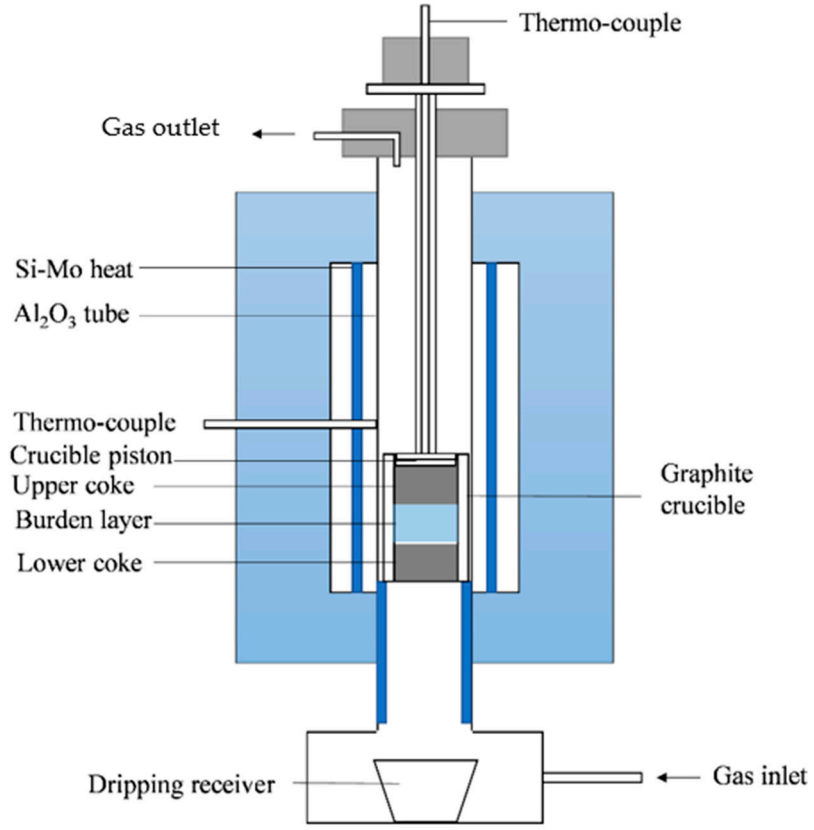

Figure 1. Soft-melting process equipment diagram.

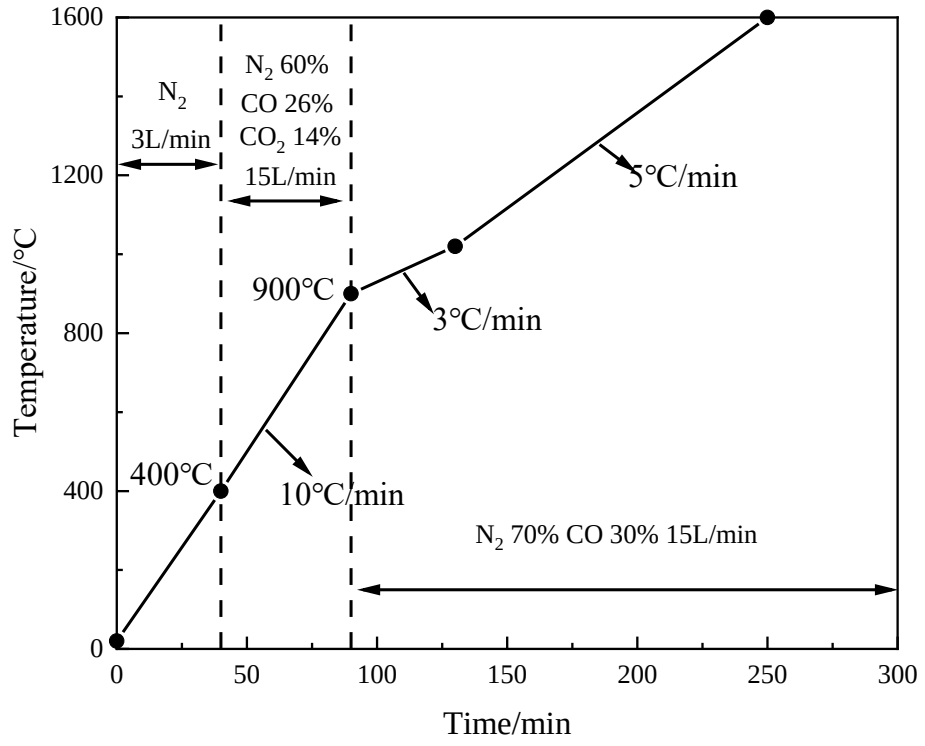

Figure 2. Temperature regime and atmosphere changes in softening-melting treatment.

3. Results and Discussion

3.1. Effect of V_2O_5 on the Properties of High-Cr VTM Pellets

The performance of the green pellets with different V_2O_5 dosages is shown in Figure 3. With the increase in V_2O_5 dosages, the falling strength of green pellets was 5.3 times/pellet without V_2O_5, which then decreased to 4.8 times/pellet at 6% with the increase in V_2O_5 dosages, and then raised to 7.6 times/pellet at 9% V_2O_5 dosages. Falling strength was all ≥3 times/pellet. The compressive strength showed a trend of first increasing and then decreasing and the lowest was 9.98 N/pellet when the V_2O_5 proportion was 3%, which was still ≥9 N/pellet. In summary, the falling strength and compressive strength of green pellets met the basic requirements. The moisture content of green pellets was about 8%, which was consistent with the best green pellets.

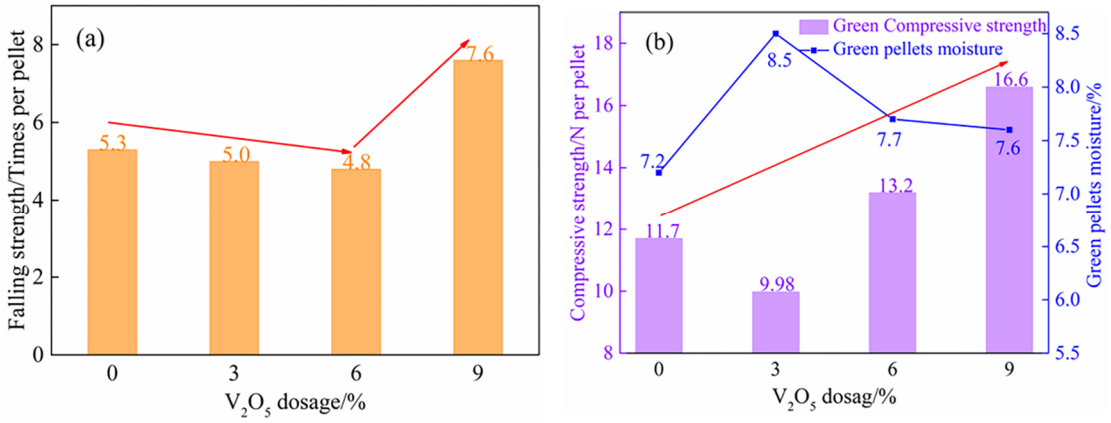

Figure 3. Effect of V_2O_5 content on the performance of green pellets. (**a**) Falling strength; (**b**) Compressive strength and moisture.

The performance of green pellets depends on many factors, including the moisture and time of forming the pellets, the particle size and surface characteristics of the raw materials, and additives [28,29]. The coarse particle size of High-Cr VTM led to poor pellet-forming performance and had a certain effect on the bonding between powder particles in the pelletizing process but the effect was not significant. With the increase in V_2O_5 addition, the number of small particles in the mixture increased, and the particle fillers in green pellets became denser, which made the strength of the green pellet increase [30–32].

3.2. Effect of V_2O_5 on Compressive Strength of High-Cr VTM Pellets

The compressive strength of oxidized pellets with different V_2O_5 contents is shown in Figure 4. The compressive strength of oxidized pellets without V_2O_5 was 3132 N/pellet. With the increase in V_2O_5 content, the compressive strength of finished pellets first decreased by a small amount and then increased rapidly. It increased from 2565 N/pellet at 6% to 3941 N/pellet at 9%. When the dosage was 6%, it reduced to 2565 N/pellet but it was still higher than 2000 N/pellet, which met the quality requirements of blast furnace production for pellets.

XRD analysis was conducted on oxidized pellets with different V_2O_5 contents and the results are shown in Figure 5. The figure shows that Fe existed in the finished oxidized pellets in the form of Fe_2O_3, $(Fe_{0.6}Cr_{0.4})_2O_3$, and $Fe_2Ti_3O_9$. The possible reaction is shown in Equation (3).

$$4Fe_3O_4 + O_2 = 6Fe_2O_3 \quad (3)$$

Fe_3O_4 reacted with O_2 to form Fe_2O_3. The existing form of Ti was mainly $Fe_2Ti_3O_9$ after roasting with Fe, the existing form of Cr was mainly $(Fe_{0.6}Cr_{0.4})_2O_3$, the existing form

of V was mainly $CrVO_3$, the existing form of V was mainly V_2O_3 after adding V_2O_5, and the possible reaction is shown in Equation (4).

$$4Fe_3O_4 + V_2O_5 = 6Fe_2O_3 + V_2O_3 \quad (4)$$

The compressive strength of oxidized pellets mainly depends on the internal microstructure of pellets during oxidation roasting and consolidation. In order to further investigate the influence of V_2O_5 on the compressive strength of oxidized pellets, Scanning Electron Microscope (SEM) (Ultra Plus; Carl Zeiss GmbH, Jena, Germany) was used to analyze the microstructure of oxidized pellets, and the results are shown in Figure 6.

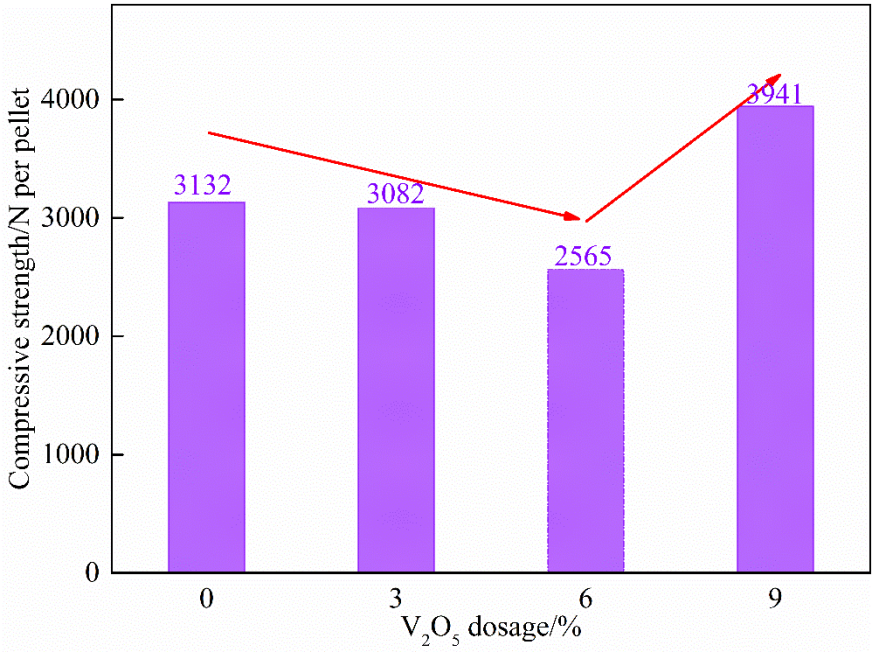

Figure 4. Influence of V_2O_5 content on compressive strength of finished oxidized pellets.

Figure 4 shows that the compressive strength of oxidized pellets first decreased and then increased with the increase in V_2O_5. As can be seen from Figure 6, the oxidized pellets without V_2O_5 had tight internal structures, few pores, small pore sizes, and uniform pore distribution. The white Fe_2O_3 crystal had an arc-shaped around the grain, the grain was coarse, the connection between the grains was closer, and the consolidation was better. All these led to a higher compressive strength of oxidized pellets when the V_2O_5 dosage was 0%. After the addition of V_2O_5, the internal structure of the oxidized pellets was obviously different from that of the oxidized pellets without V_2O_5, with significantly more pores and larger pore sizes and dispersed distribution. As can be seen from the EDS diagram at point B in Figure 7, the black ones were free Si and O phases, and the dispersed distribution of Si and O phases between the Fe_2O_3 crystals led to a poor bonding force and looser structure of Fe_2O_3. As can be seen from Figure 7, after the addition of V_2O_5, the adhesion of the vanadium phase between and on crystals reduced the crystallization effect of Fe_2O_3 crystals, all of which reduced the compressive strength of oxidized pellets containing V_2O_5. As can be seen from Figure 6, the pore size with the addition of 6%V_2O_5 was larger and the distribution was more dispersed than that with the addition of 3%V_2O_5, so the strength of the oxidized pellets of 6% was lower than that of 3%. The liquid phase generated by the continuous addition of V_2O_5 in 9% oxidized pellets had an enhanced effect on the compressive strength of the pellets. When the enhanced effect of the liquid phase exceeded the inhibition effect of the addition of V_2O_5 on the crystallization effect of Fe_2O_3 crystals, the compressive strength of pellets gradually increased; therefore, the compressive strength of oxidized pellets decreased first and then increased with the increase in V_2O_5.

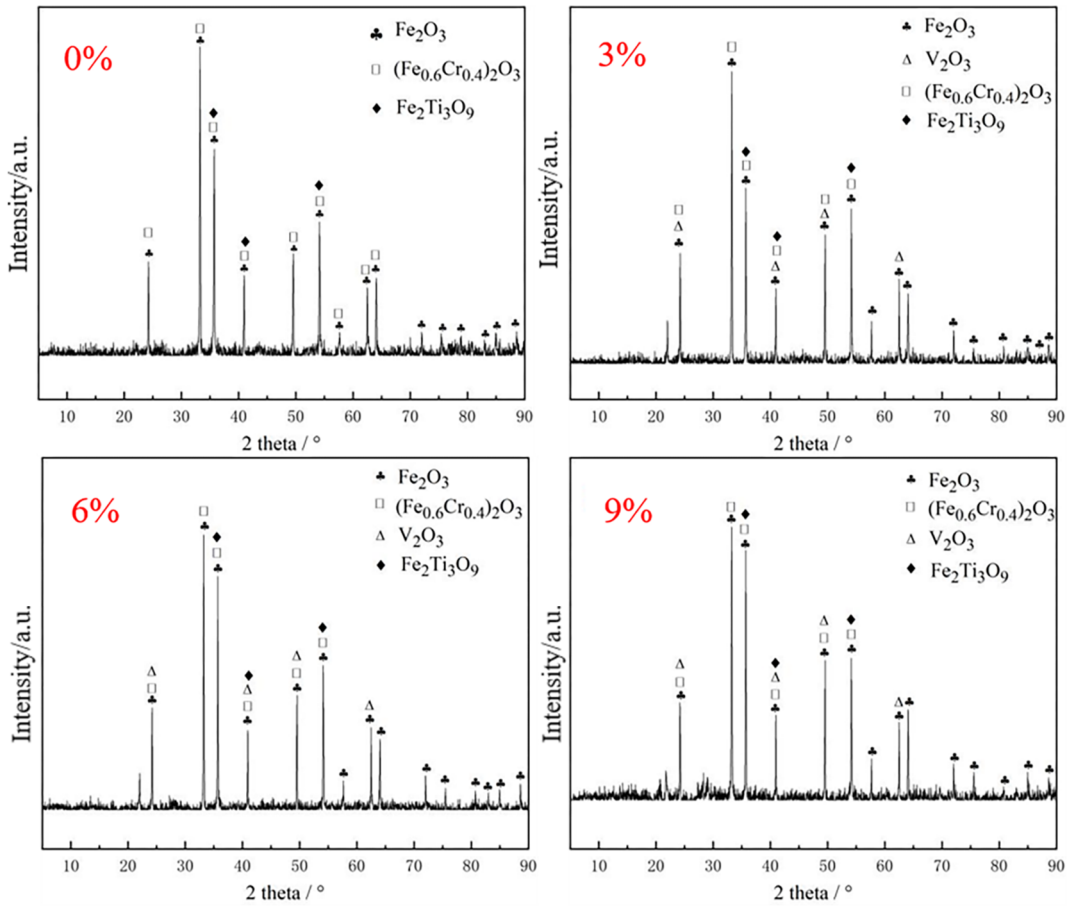

Figure 5. X-ray diffraction pattern of oxidized pellets.

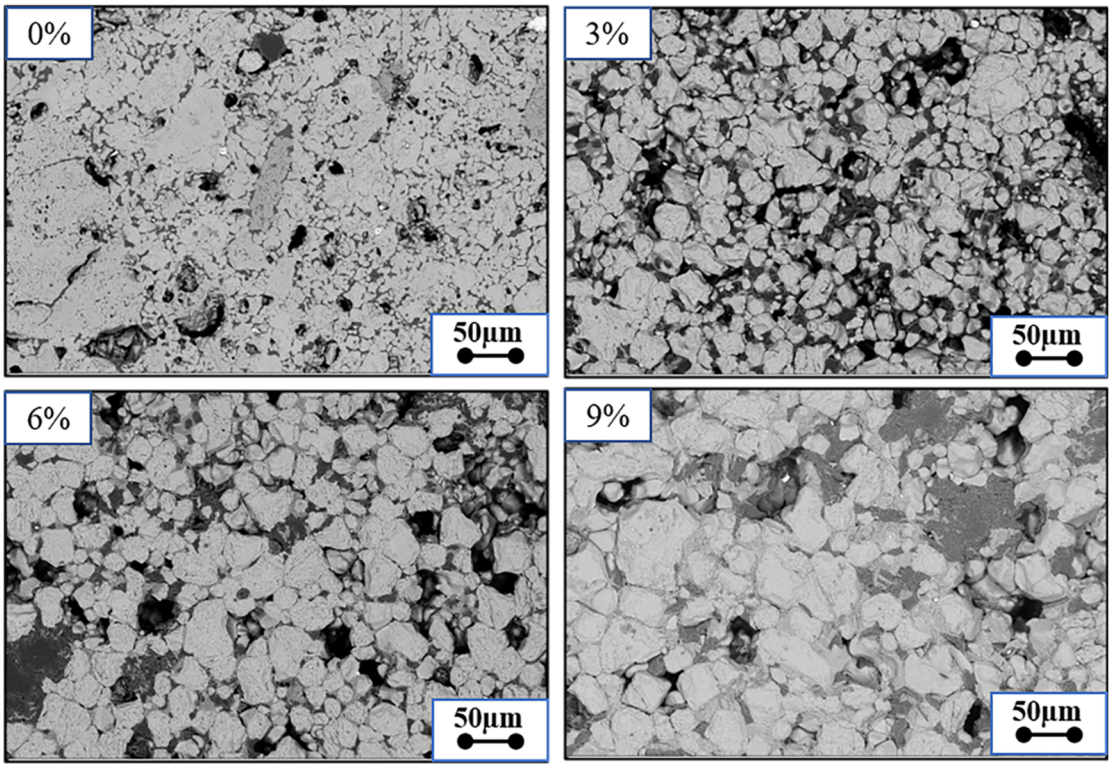

Figure 6. Microstructure of oxidized pellets.

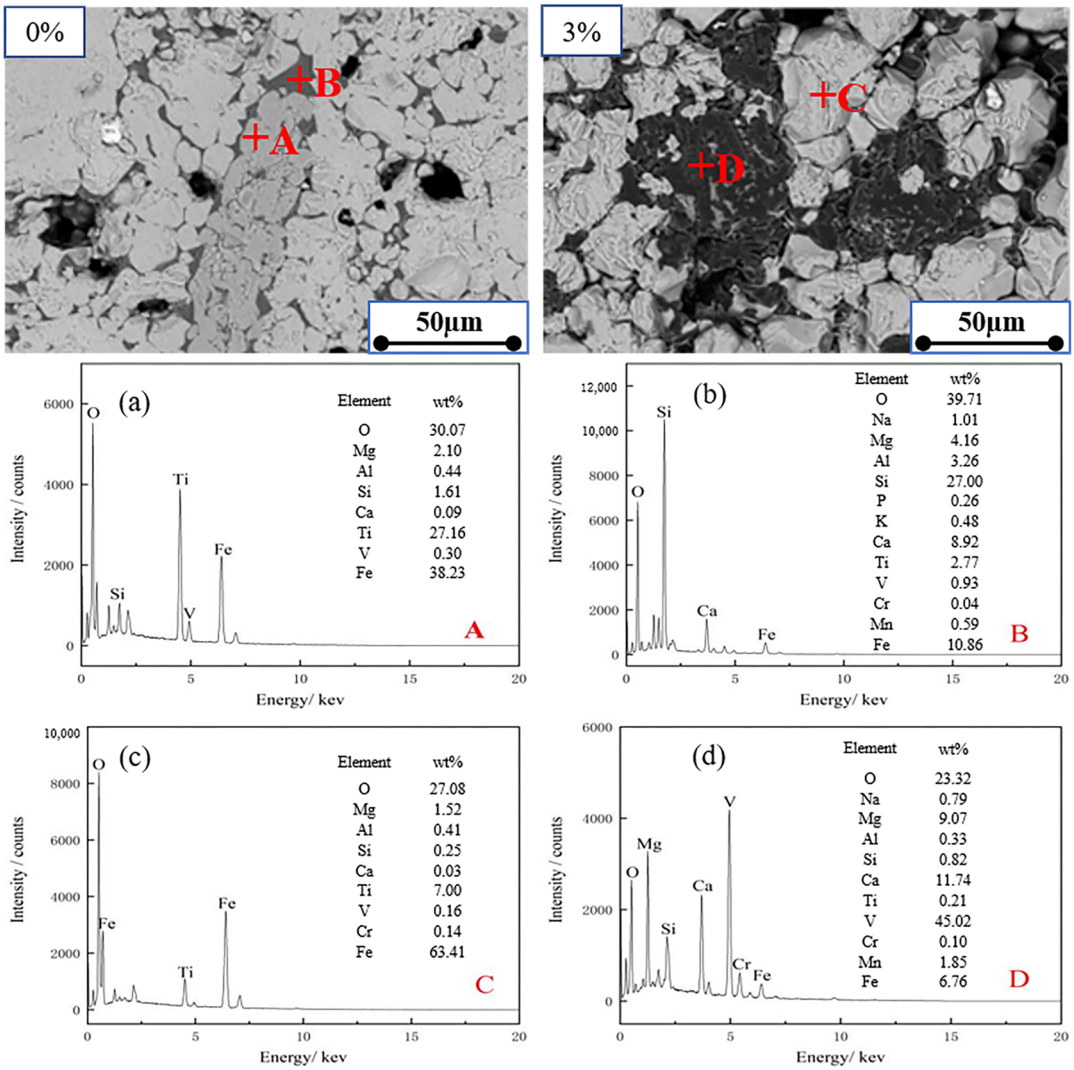

Figure 7. SEM–EDS analysis of oxidized pellets containing V_2O_5. (**a**) Point A; (**b**) Point B; (**c**) Point C; (**d**) Point D.

3.3. Effect of V_2O_5 on Pellet Reduction Swelling Index

The effects of different V_2O_5 dosages on the reduction swelling index and the compressive strength of the swelling pellets are shown in Figure 8. As can be seen from Figure 8, the reduction swelling index of pellets first increased and then decreased with the increase in V_2O_5 dosage. Without V_2O_5, the reduction swelling index of pellets was 10.42%. When the V_2O_5 dosage was increased to 3%, the reduction swelling index of pellets was increased to 14.76%; however, with the increase in V_2O_5 dosage, the reduction swelling index of pellets began to decrease. At the same time, the compressive strength of pellets reduced by adding V_2O_5 was much lower than that of pellets without adding V_2O_5, which decreased from 1313 N/pellet of 0% V_2O_5 to 182 N/pellet of 3%, while the strength of 3%, 6%, and 9% pellets did not change much.

Figure 9 shows the X-ray diffraction analysis of reduced pellets. As can be seen from Figure 9, Fe_2O_3 was reduced into Fe_3O_4, FeO, and elemental Fe in the reduction process. The existing form of Ti after reduction was $Fe_{2.75}Ti_{0.25}O_4$, and the existing form of Cr after reduction was $FeCr_2O_4$. Meanwhile, the peak value of elemental iron was the highest in the four groups when the V_2O_5 dosage was 3%, which proved that the reduction degree reached the highest when the V_2O_5 dosage was 3%; this was also consistent with the changing trend of the reduction swelling index shown in Figure 8.

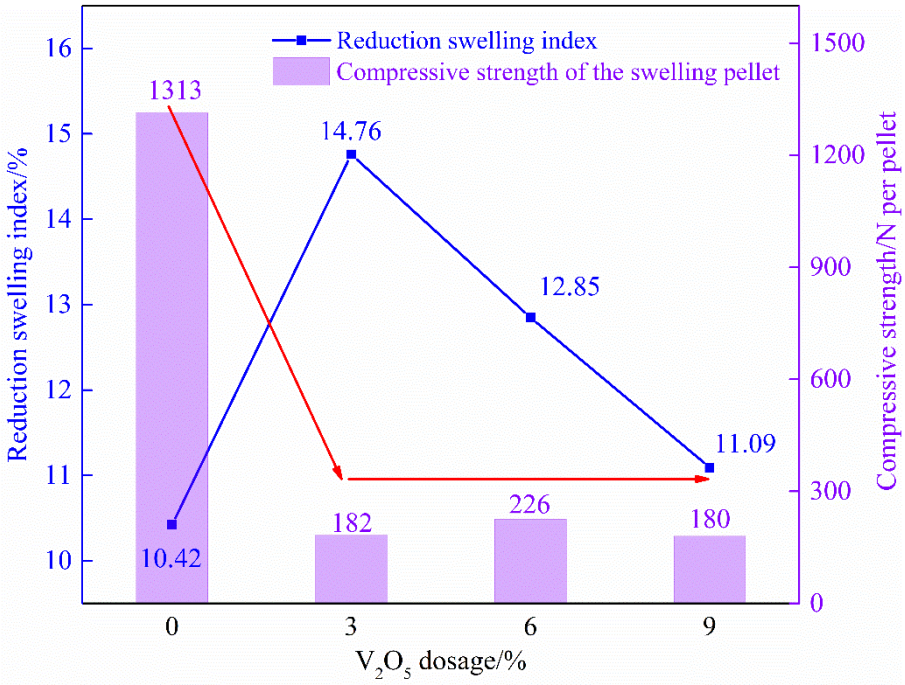

Figure 8. Effects of V_2O_5 dosage on the reduction swelling index of the oxidized pellets and compressive strength of the swelling pellets.

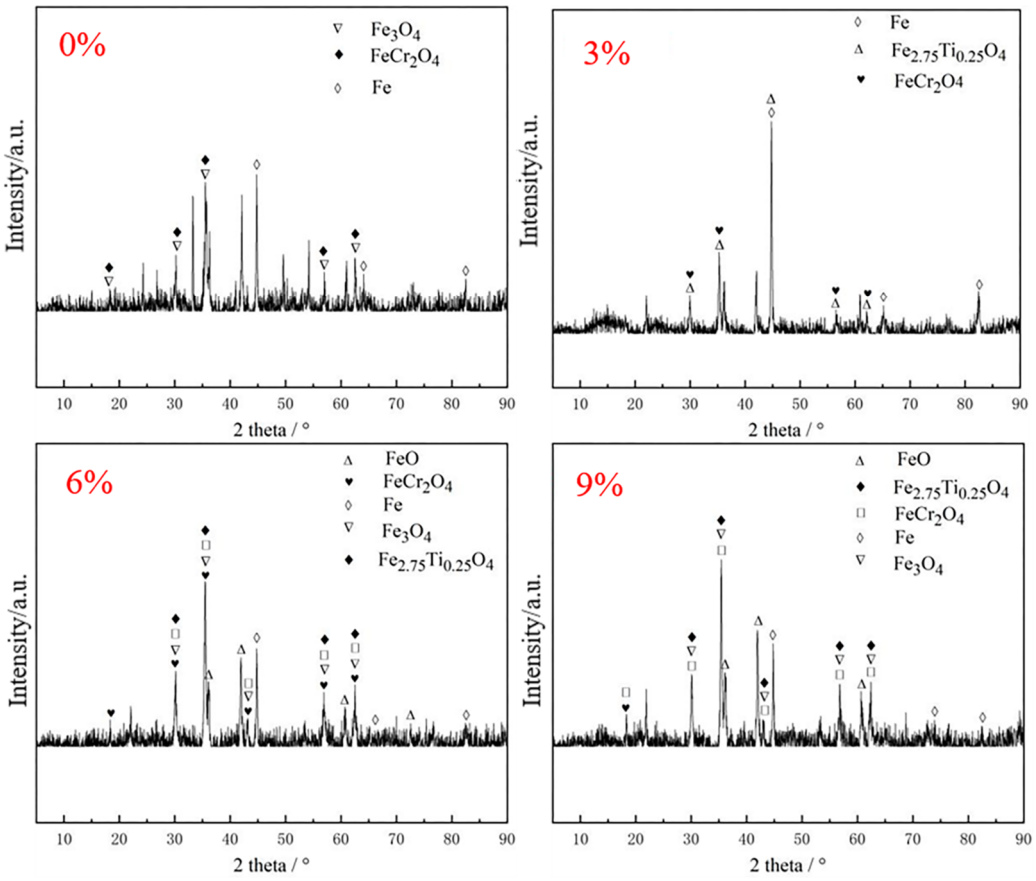

Figure 9. X-ray diffraction analysis of reduced pellets.

Figure 10 shows the microstructure of pellets after reduction. There were many iron whiskers inside pellets containing V_2O_5 after reduction, which hindered the passage of

reducing gas and deteriorated the reduction effect; therefore, the reduction swelling index showed a downward trend after 3% V_2O_5. At the same time, these iron whiskers made the internal structure of the pellets looser, so the compressive strength of the reduced pellets containing V_2O_5 was much lower than that of pellets without V_2O_5. When the V_2O_5 dosage was 6%, the reduced iron crystals inside the pellets were lamellar.

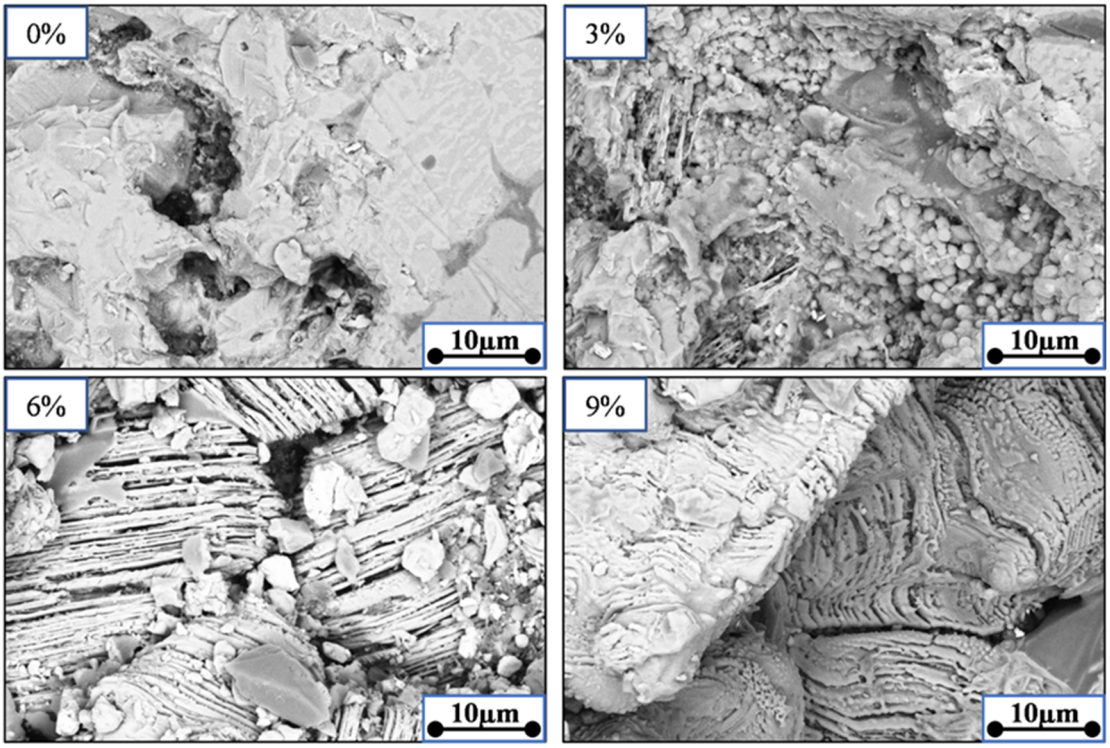

Figure 10. SEM of reduced pellets at 900°C for 60min.

With the increase in V_2O_5 dosage, the reduction degree of the pellets increased first and then decreased, and the increased speed of the reduction degree was faster than the decreasing trend as shown in Figure 11. When the dosage of V_2O_5 was 3%, the reduction degree of the pellets reached the highest, 72.56%. The reason why the reduction degree first increased and then decreased was that when there was a large amount of V_2O_5, many iron whiskers were generated during the reduction process of the pellets, which hindered the passage of reducing gas and made the reduction effect worse; therefore, the reduction degree of the pellets first increased and then decreased.

3.4. Effect of V_2O_5 on Soft Melting–Dripping Properties of High-Cr VTM Pellets

Figure 12 shows the effect of V_2O_5 dosage on the softening-melting behavior of High-Cr VTM pellets. With the increase in the dosages of V_2O_5, the softening initial temperature, softening final temperature, melting initial temperature, and the dropping temperature of High-Cr VTM pellets increased gradually; especially when 3% V_2O_5 was added, the initial softening temperature increased from 936 °C to 1075 °C, the melting temperature from 1063 °C to 1184 °C, and the dropping temperature from 1190 °C to 1464 °C. The melting interval decreased from 88 °C to 57 °C when the mass fraction of V_2O_5 increased from 0% to 6%, and the melting interval increased from 127 °C to 280 °C when the mass fraction of V_2O_5 increased from 0% to 3%.

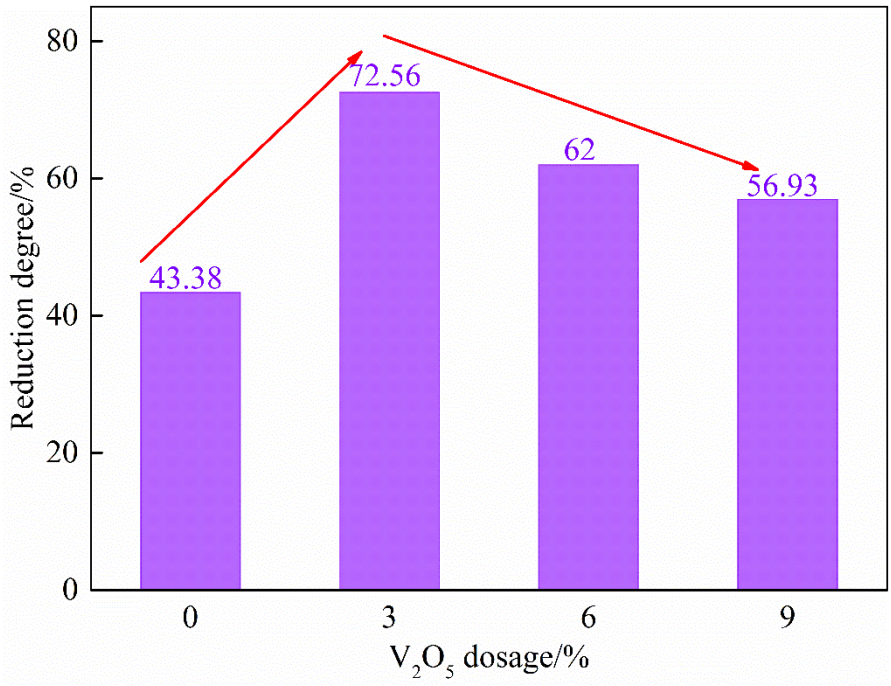

Figure 11. Effect of V_2O_5 dosage on reduction degree of pellets.

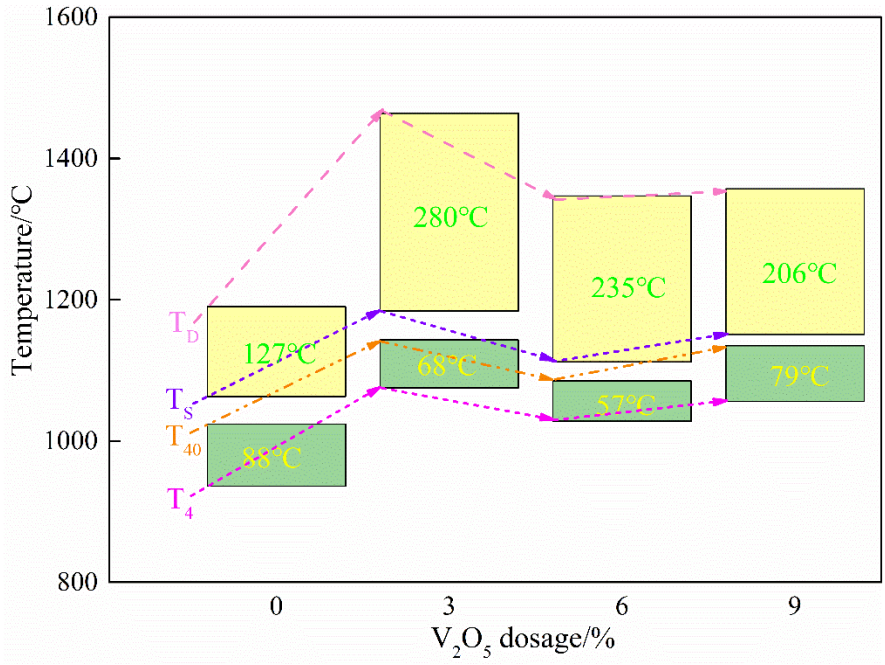

Figure 12. Effect of V_2O_5 dosage on softening-melting behavior of High-Cr VTM pellets.

In the process of blast furnace smelting, increasing the initial softening temperature and narrowing the softening interval is helpful to keep the furnace condition stable for the gas–solid reduction reaction [15–18]. In this study, when the V_2O_5 mass fraction increased from 0% to 6%, the softening initial temperature increased and the softening interval narrowed, which was conducive to improving the reduction melting index in the soft melting dripping process; however, as the mass fraction of V_2O_5 continued to increase to 9%, the softening initial temperature increased and softening characteristics improved. The softening index deteriorated with the increase in softening interval thickness. With the increase in the V_2O_5 dosage in pellets, the reduction of V_2O_3 content increased, and

vanadium oxide combined with iron oxide also gradually increased, $FeO{\cdot}V_2O_3$ was easy to be reduced to V_2O_3, Fe, and CO_2, and these reactions had a certain impact on the softening temperature. The droplet characteristics can be improved by increasing the initial melting temperature and narrowing the droplet interval [18,19]. In this study, with the mass fraction of V_2O_5 increasing from 0% to 3%, the increase in melting temperature was beneficial to the enhancement of the blast furnace (BF) smelting index; however, the melting drop interval was rapidly enlarged to 280 °C, which made the BF melting index worse. When the mass fraction of V_2O_5 increased from 3% to 9%, the range of melting droplets became narrower, which was beneficial to blast furnace smelting; meanwhile, the melting start temperature decreased, which was not conducive to blast furnace smelting.

The chemical composition of the undripped and the dripped materials obtained after the soft melting dripping experiment was analyzed, and the results are listed in Tables 3 and 4. During the formation of slag iron, the content of V_2O_5 in pellets had a certain influence on the migration of valuable components Cr, V, and Ti. With the increase in V_2O_5 content, the content of V and Cr in the iron were increased overall, and the content of Ti in the slag was higher, which proved that Cr and V obtained by reduction were more likely to migrate to the molten iron, and the titanium was transferred to the slag in the form of titanium oxide [33].

Table 3. Effect of V_2O_5 on the chemical composition of the slag after soft melting dripping.

V_2O_5 Dosage	MgO/%	CaO/%	SiO_2/%	Al_2O_3/%	TiO_2/%
0%	8.32	1.89	16.32	5.95	21.36
3%	6.18	1.95	18.92	7.17	14.27
6%	4.68	1.90	17.48	5.87	12.48
9%	2.06	2.06	18.95	8.19	15.87

Table 4. Effects of V_2O_5 on the content of vanadium and chromium in the dribbling iron after soft melting of High-Cr VTM pellets.

V_2O_5 Dosage	V/%	Cr/%
0%	0.016	0.028
3%	0.569	0.088

Figure 13 shows the SEM–EDS diagram of the slag from soft melting–dripping of High-Cr VTM with V_2O_5 mass fractions of 3% and 6%. The bright white area was the iron phase, the oxides of titanium and vanadium at points A and C, and the slag phase at points B and D. With the increase in V_2O_5 mass fraction from 3% to 6%, the iron phase in the slag obtained from soft melting drips of High-Cr VTM pellets changed from round shape to group shape, and the shape of vanadium oxides and titanium oxides changed from round spot shape and round strip shape to irregular polygonal flake, and the size, quantity, and degree of aggregation became larger. With the increase in V_2O_5 mass fraction, the content of vanadium oxide increased and the content of titanium oxide decreased in the slag obtained from the soft melting of the pellets, which was consistent with the result of the gradual decrease in TiO_2 content observed in the previous studies on the migration behavior of valuable components [17–19].

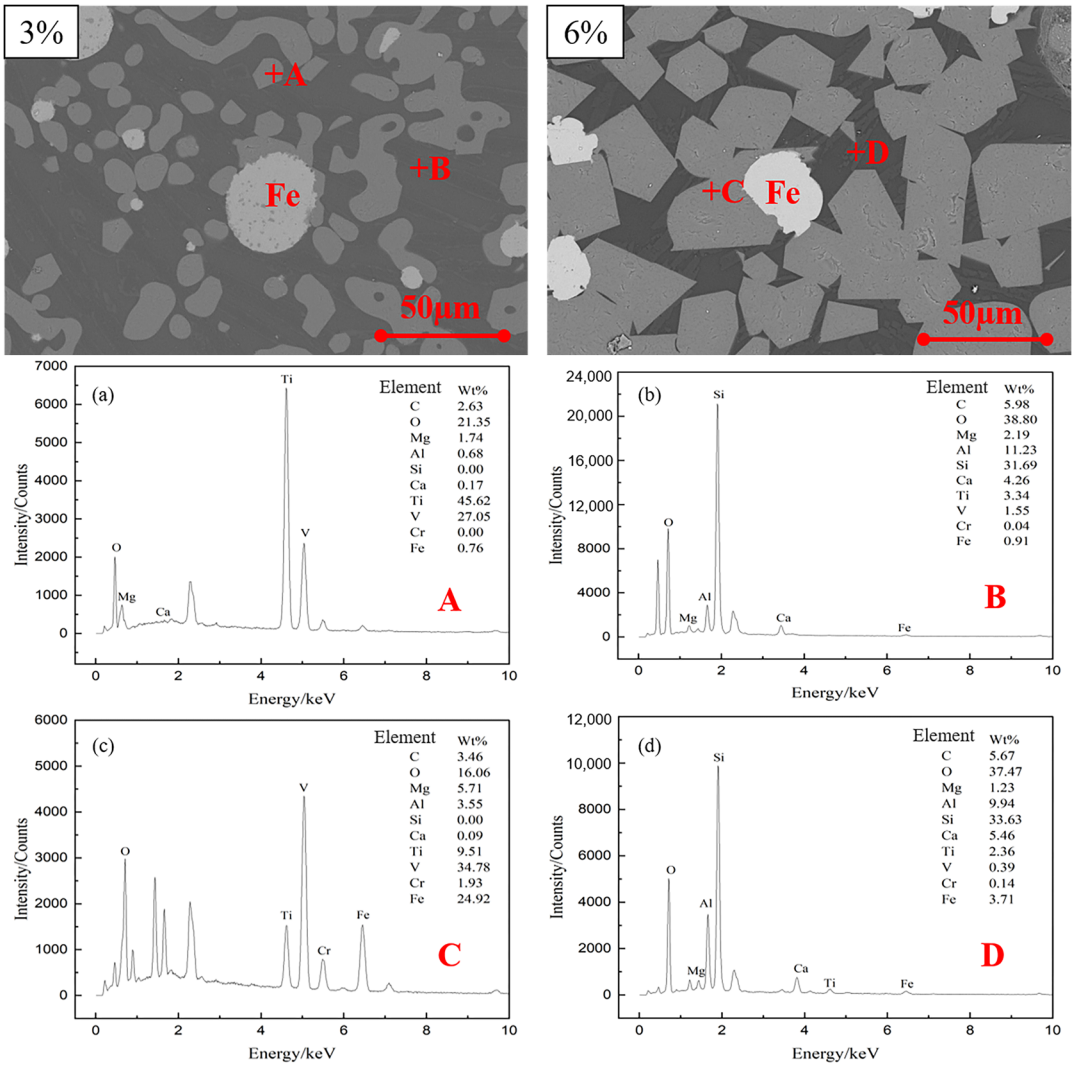

Figure 13. SEM–EDS diagram of soft melting–dripping slag of High-Cr VTM pellets with V_2O_5 mass fractions of 3% and 6%. (**a**) Point A; (**b**) Point B; (**c**) Point C; (**d**) Point D.

Figure 14 shows the SEM–EDS diagram of dripping iron of High-Cr VTM pellets with V_2O_5 mass fractions of 6% and 9%. Points A and C were the iron phase and points B and D were the carbon. The results showed that with the increase in V_2O_5 content, the carbon content in the dripping iron gradually increased, and the size also increased, indicating excess carbon, which did not complete the reaction. As seen in the energy spectrum analysis diagrams A and C, as the iron drops melted, the presence of carbon in the iron phase increased, which further indicated an excess of carbon. By studying the element storage of drip iron in pellets with different V_2O_5 contents, it was found that the content of titanium in drip iron was at a relatively low level, which further verified the view that Ti was more easily transferred to slag.

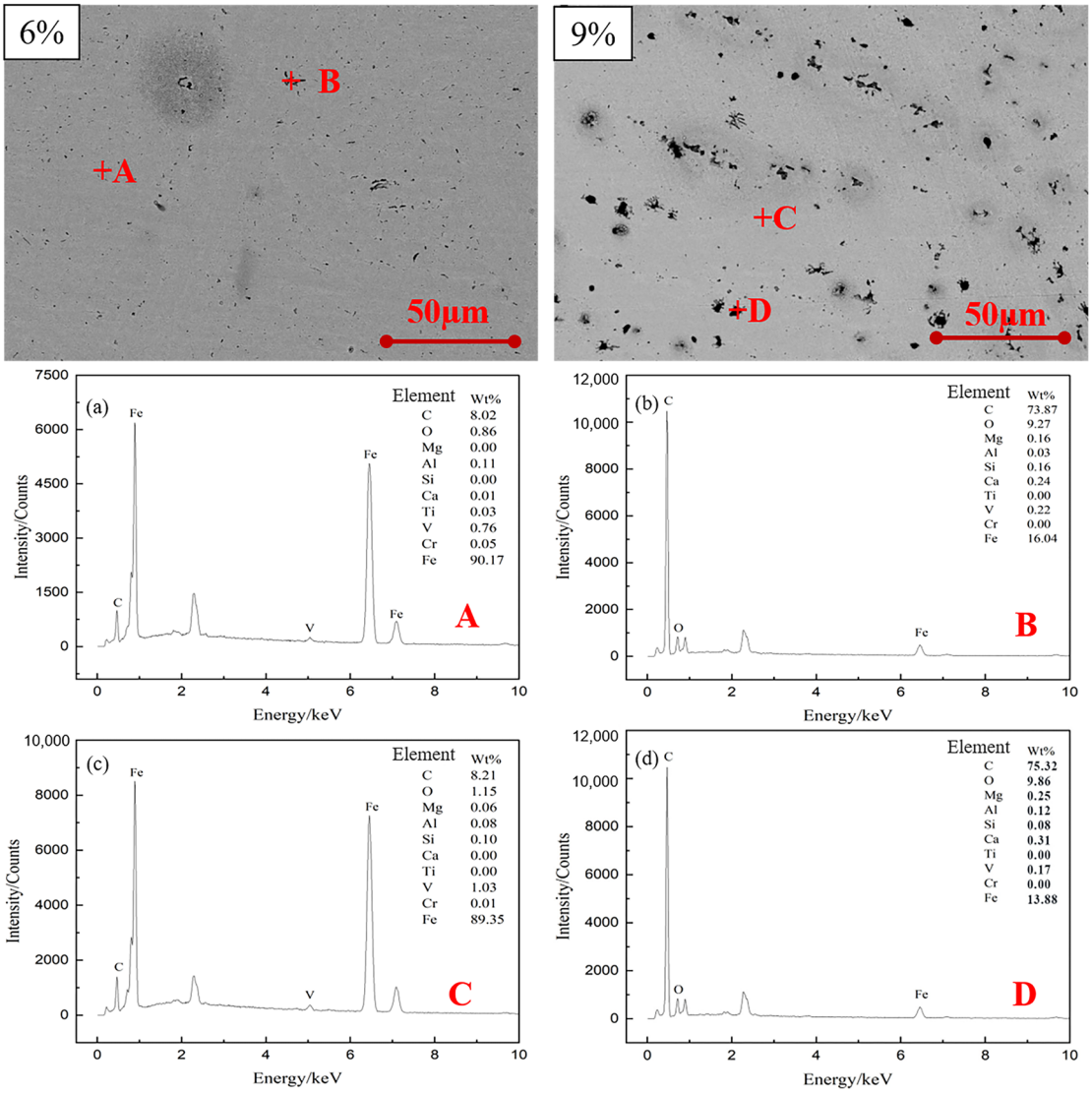

Figure 14. SEM–EDS diagram of dripping iron of High-Cr VTM pellet with V_2O_5 mass fractions of 6% and 9%. (**a**) Point A; (**b**) Point B; (**c**) Point C; (**d**) Point D.

4. Conclusions

(1) Under the experimental conditions of this study, V_2O_5 had little effect on the performance of green pellets and oxidized pellets. The performance of green pellets basically showed a trend of first decreasing and then increasing but the change was not great, and all met the basic requirements of pellets. When the V_2O_5 content was 6%, the compressive strength of pellets was the lowest, at 2565 N/pellet, which met the quality requirement of pellets in blast furnace production;

(2) The addition of V_2O_5 worsened the swelling of the pellets. With the increase in V_2O_5 content, the reduction swelling index and reduction degree of finished pellets were first increasing and then decreasing; both reached the highest when the V_2O_5 content was 3% and deteriorated more seriously when the V_2O_5 content was less than 3%. When the V_2O_5 content was greater than 3%, the deterioration effect decreased with the increase in V_2O_5 content;

(3) The addition of V_2O_5 reduced the compressive strength of the reduced pellets. The compressive strength of the finished pellet with V_2O_5 after reduction was about 200 N/pellet, which was much lower than that of the finished pellet without V_2O_5 with 1313 N/pellet;

(4) The addition of V_2O_5 increased the softening initial temperature, softening final temperature, melting start temperature, and dripping temperature of High-Cr VTM pellets, so that the softening interval became narrower and the melting drop interval became wider. From the view of softening performance, the addition of V_2O_5 was conducive to improving the reduction melting index of the melting–dripping process, which was conducive to blast furnace smelting. In the process of droplet and separation of slag iron, V and Cr were easy to migrate into iron, while Ti was easier to migrate into slag.

Author Contributions: Conceptualization, X.X.; methodology, Z.X.; validation, Z.X. and X.X.; formal analysis, X.W.; investigation, G.C.; resources, X.X.; data curation, G.C. and Z.X.; writing—original draft preparation, J.L. and X.W.; writing—review and editing, G.C. and Z.X.; supervision, X.X.; project administration, X.X.; funding acquisition, J.L. and X.X. All authors have read and agreed to the published version of the manuscript.

Funding: This work was supported by the National Natural Science Foundation of China (Grant No. 22008027, U1908226).

Data Availability Statement: Not applicable.

Conflicts of Interest: The authors declare no conflict of interest.

References

1. Jung, S.M. Effects of $CaO/CaCO_3$ on the carbothermic reduction of titanomagnetite ores. *Metall. Mater. Trans. B* **2015**, *46*, 1162–1174. [CrossRef]
2. Xing, Z.X.; Liu, J.S.; Cheng, G.J.; Yang, H.; Xue, X.X. Migration Behavior of Valuable Components in Pellets with Sea Sand Vanadium Titanomagnetite During the Oxidation Roasting Process. *JOM* **2023**, *75*, 1–10. [CrossRef]
3. Prabowo, S.W.; Longbottom, R.J.; Monaghan, B.J.; Puerto, D.; Ryan, M.J.; Bumby, C.W. Phase transformations during fluidized bed reduction of New Zealand titanomagnetite ironsand in hydrogen gas. *Powder Technol.* **2021**, *398*, 117032–117047. [CrossRef]
4. Tang, W.D.; Yang, S.T.; Zhang, L.H.; Huang, Z.; Yang, H.; Xue, X.X. Effects of basicity and temperature on mineralogy and reduction behaviors of high-chromium vanadium-titanium magnetite sinters. *J. Cent. South Univ.* **2019**, *26*, 132–145. [CrossRef]
5. Jena, B.C.; Dresler, W.; Reilly, I.G. Extraction of titanium, vanadium and iron from titanomagnetite deposits at pipestone lake, Manitoba, Canada. *Miner. Eng.* **1995**, *8*, 159–168. [CrossRef]
6. Liu, J.X.; Cheng, G.J.; Liu, Z.G.; Chu, M.S.; Xue, X.X. Reduction process of pellet containing high chromic vanadium–titanium magnetite in cohesive zone. *Steel Res. Int.* **2015**, *86*, 808–816. [CrossRef]
7. Xing, Z.X.; Ma, J.; Cheng, G.J.; Yang, H.; Xue, X.X. Study on the High-Temperature Sintering Characteristics and Sintering Mechanism of Sea Sand Vanadium Titanomagnetite Based on Micro-sintering. *J. Sustain. Metall.* **2022**, *8*, 1358–1369. [CrossRef]
8. Yan, W.P.; Zeng, X.B. Study on the Evaluation Method of Development and Utilization Level of Vanadium-titanium Magnetite Mine in Panxi District. *Multipurp. Util. Miner. Resour.* **2020**, *226*, 79–83.
9. Xing, Z.X.; Huang, Z.; Cheng, G.J.; Yang, H.; Xue, X.X.; Zhang, G.D. Comprehensive evaluation of high-temperature sintering behavior of sea sand vanadia-titania magnetite based on grey relational analysis. *Korean J. Chem. Eng.* **2022**, *39*, 3464–3472. [CrossRef]
10. Xue, Y.Z.; Wang, X.F.; Wang, H.J.; Li, W.C. On Comprehensive Utilization of Vanadium-Titanium Magnetite Resources in Panxi Region of Sichuan Province. *Nat. Resour. Econ. China* **2017**, *30*, 9–13.
11. Cheng, H.B.; Zhou, Z.H.; Zhang, Z.J.; Zhang, Z.F.; Yang, S.F. Research Progress in the Comprehensive Recovery of Vanadium-Titanium Magnetite. *Mod. Min.* **2023**, *39*, 7–9.
12. Wu, E.H.; Li, J.; Xu, Z.; Hou, J.; Huang, P. Physicochemical Properties of Metallized Pellets of High-Chromium Vanadium-bearing Titanomagnetite. *Iron Steel* **2023**, *58*, 30–38.
13. Tang, J.; Chu, M.S.; Feng, C.; Li, F.; Tang, Y.T.; Liu, Z.G. Melting Separation Process of High Chromium Vanadium-bearing Titanomagnetite Metallized Pellet, and its Optimization by Multi-Index Synthetic Weighted Scoring Method. *ISIJ Int.* **2017**, *57*, 1156–1165. [CrossRef]
14. Tang, J.; Chu, M.S.; Feng, C.; Tang, Y.T.; Liu, Z.G. Melting Separation Behavior and Mechanism of High-chromium Vanadium-bearing Titanomagnetite Metallized Pellet Got from Gas-based Direct Reduction. *ISIJ Int.* **2016**, *56*, 210–219. [CrossRef]
15. Zhang, L.H.; Gao, Z.X.; Yang, S.T.; Tang, W.D.; Xue, X.X. Effect of basicity on sintering behavior and metallurgical properties of high-chromium vanadium-titanium magnetite. *Metals* **2020**, *10*, 569. [CrossRef]
16. Zhang, L.H.; Yang, S.T.; Tang, W.D.; Xue, X.X. Investigations of MgO on sintering performance and metallurgical property of high-chromium vanadium-titanium magnetite. *Minerals* **2019**, *9*, 324. [CrossRef]
17. Cheng, G.J.; Gao, Z.X.; Yang, H.; Xue, X.X. Effect of Calcium Oxide on the Crushing Strength, Reduction and Smelting Performance of High Chromium Vanadium Titanium Magnetite Pellets. *Metals* **2017**, *7*, 181. [CrossRef]

18. Cheng, G.J.; Xue, X.X.; Gao, Z.X.; Jiang, T.; Yang, H.; Duan, P.N. Effect of Cr_2O_3 on the Reduction and Smelting Mechanism of High-Chromium Vanadium-titanium Magnetite Pellets. *ISIJ Int.* **2016**, *56*, 1938–1947. [CrossRef]
19. Cheng, G.J.; Xue, X.X.; Jiang, T.; Duan, P.N. Effect of TiO_2 on the Crushing Strength, and Smelting Mechanism of High-Chromium Vanadium-Titanium Magnetite Pellets. *Metall. Mater. Trans. B* **2016**, *47*, 1713–1726. [CrossRef]
20. Cheng, G.J.; Liu, J.X.; Liu, Z.G.; Chu, M.S.; Xue, X.X. Non isothermal Reduction Kinetics and Mechanism of High Chromium Vanadium Titanium Magnetite Pellets. *Ironmak. Steelmak.* **2015**, *42*, 17–26. [CrossRef]
21. Cheng, G.J.; Gao, Z.X.; Lv, M.Y.; Yang, H.; Xue, X.X. Coal based Reduction and Magnetic Separation Behavior of Low-grade Vanadium Titanium Magnetite Pellets. *Minerals* **2017**, *7*, 86. [CrossRef]
22. Li, F.; Chu, M.S.; Tang, J.; Liu, Z.G.; Feng, C.; Tang, Y.T. Swelling Behavior of High-Chromium, Vanadium-Bearing Titanomagnetite Pellets in H2-CO-CO2 Gas Mixtures. *JOM* **2017**, *69*, 1751–1758. [CrossRef]
23. Zhou, M.; Yang, S.T.; Jiang, T.; Xue, X.X. Influence of basicity on high chromium vanadium-titanium magnetite sinter properties, productivity, and mineralogy. *JOM* **2015**, *67*, 1203–1213. [CrossRef]
24. Gao, S.M. Discussion on Smelting Technology of a High Chromium Vanadium Titanium Magnetite. *Iron Steel Vanadium Titan.* **2020**, *41*, 27–36.
25. Cheng, Y. Practice on the Development and Utilization of Vanadic Titanomagnetite Resources in Panzhihua. *Iron Steel Vanadium Titan.* **2009**, *30*, 78–79.
26. Liu, Z.G.; Chu, M.S.; Wang, H.T.; Zhao, W.; Xue, X.X. Effect of MgO content in sinter on the softening-melting behavior of mixed burden made from chromium-bearing vanadium–titanium magnetite. *Int. J. Miner. Metall. Mater.* **2016**, *23*, 25–32. [CrossRef]
27. Zeng, R.Q.; Wang, N.; Li, W. Non-isothermal oxidation induration mechanism of vanadium titanomagnetite pellets. *Adv. Powder Technol.* **2023**, *34*, 104012. [CrossRef]
28. Xing, Z.X.; Cheng, G.J.; Gao, Z.X.; Yang, H.; Xue, X.X. Optimization of experimental conditions on preparation of oxidized pellets with New Zealand sea sand ore. *Metall. Res. Technol.* **2020**, *117*, 411–421. [CrossRef]
29. Xing, Z.X.; Cheng, G.J.; Yang, H.; Xue, X.X. Experimental Research on Preparation of Oxidized Pellets with High Proportion Sea Sand Mine. In Proceedings of the 12th CSM Steel Congress, Beijing, China, 14–16 October 2019; pp. 1–4.
30. Xing, Z.; Huang, Z.; Cheng, G.; Yang, H.; Xue, X. Consolidation, and reduction behavior of pellets with sea sand vanadium titanomagnetite: A microscopic interpretation of macroscopic properties. *Ironmak. Steelmak.* **2022**, 1–11. [CrossRef]
31. Cheng, G.J.; Xing, Z.X.; Yang, H.; Xue, X.X. Effects of High Proportion Unground Sea Sand Ore on the Preparation Process and Reduction Performance of Oxidized Pellets. *Minerals* **2021**, *11*, 87. [CrossRef]
32. Xing, Z.; Cheng, G.; Gao, Z.; Yang, H.; Xue, X. Effect of Incremental Utilization of Unground Sea Sand Ore on the Consolidation and Reduction Behavior of Vanadia-Titania Magnetite Pellets. *Metals* **2021**, *11*, 269. [CrossRef]
33. Wang, S.; Guo, Y.F.; Zheng, F.Q.; Chen, F.; Yang, L.Z.; Jiang, T.; Qiu, G.Z. Behavior of vanadium during reduction and smelting of vanadium titanomagnetite metallized pellets. *Tran. Nonferr. Metals Soc. China* **2020**, *30*, 1687–1696. [CrossRef]